DFT calculations, crystal structure, Hirshfeld surface analyses and antibacterial studies of a new tetrachlorocuprate salt: (C 6 H 16 N 2 O)[CuCl 4]

Bejaoui, Chaima ; Ameur, Iness ; Derbel, Najoua ; Linden, Anthony ; Abid, Sonia

Abstract: A novel tetrachlorocuprate salt (C6H16N2O)[CuCl4] was synthesized and its crystal structure determined by single crystal X-ray diffraction analysis. This compound crystallizes in the monoclinic space group Pn with unit cell parameters a = 7.71302(11), b = 6.33580(8), c = 13.10453(19)Å, = 104.9526(15)°, V = 618.710(15)Å3 and one cation and one anion in the asymmetric unit. Its crystal structure consists of [CuCl4]2- anions surrounded by [C6H16N2O]2+ cations. NH Cl, NH O and OH Cl hydrogen bonding interactions link the entities into a three-dimensional framework. Theoretical calculations at the DFT/B3LYP/LanL2DZ level of theory provided good consistency between the calculated and experimental vibrational spectra and with the observed geometries of the ions. Compared with reference drugs, the compound exhibited moderate activity against gram-negative bacteria, while it showed modest activity against fungal and the gram-positive strains, except for S. aureus.

DOI: https://doi.org/10.1016/j.molstruc.2018.04.003

DFT calculations, crystal structure, Hirshfeld surface analyses and antibacterial studies of a new tetrachlorocuprate salt: $(C_6H_{16}N_2O)[CuCl_4]$

Chaima Bejaoui[a], Iness Ameur[a], Najoua Derbel[b], Anthony Linden[c] and Sonia Abid[a*]

[a]Laboratoire de Chimie des Matériaux, Université de Carthage, Faculté des Sciences de Bizerte, 7021 Zarzouna, Bizerte, Tunisia,
[b]Laboratoire de Spectroscopie Atomique Moléculaire et Applications (LSAMA), Faculté des Science de Tunis, Université de Tunis El Manar, 2092, Tunis, Tunisie.
[c]Department of Chemistry, University of Zurich, Winterthurerstrasse 190, CH-8057 Zurich, Switzerland.

ABSTRACT

A novel tetrachlorocuprate salt $(C_6H_{16}N_2O)[CuCl_4]$ was synthesized and its crystal structure determined by single crystal X-ray diffraction analysis. This compound crystallizes in the monoclinic space group *Pn* with unit cell parameters *a*=7.71302(11), *b*=6.33580(8), *c*=13.10453(19)Å, β =104.9526(15)°, *V*=618.710(15)Å^3 and one cation and one anion in the asymmetric unit. Its crystal structure consists of $[CuCl_4]^{2-}$ anions surrounded by $[C_6H_{16}N_2O]^{2+}$ cations. N−H···Cl, N−H···O and O−H···Cl hydrogen bonding interactions link the entities into a three-dimensional framework. Theoretical calculations at the DFT/B3LYP/LanL2DZ level of theory provided good consistency between the calculated and experimental vibrational spectra and with the observed geometries of the ions. Compared with reference drugs, the compound exhibited moderate activity against gram-negative bacteria, while it showed modest activity against fungal and the gram-positive strains, except for S. aureus.

keywords: inorganic-organic hybrid material, tetrachlorocuprate, X-ray diffraction, Hirshfeld surface, DFT, antibacterial activity.

1.Introduction

During the last decades, inorganic-organic hybrid materials have attracted much attention owing to their special structural features and potential applications derived from their optical [1,2], electronic [3,4], and ferroelectric properties [5,6]. Among these compounds, halide-transition metal complexes, such as halocuprates, have drawn growing interest because of their structural flexibility, magnetic properties related to the interionic distances between the $[MX_n]^{y-}$ anions (M=metal, X=halogen), and the properties of the cations [7,8]. In particular, the Cu(II) ion is an attractive transition metal with a d^9 electronic system and presents a variety of coordination numbers and geometries, such as octahedral, square planar, tetrahedral and square pyramidal [9]. A variety of amines has been employed previously in the preparation of halocuprates, including aliphatic, aromatic and cyclic amines [10-13]. In particular, protonated N-heterocyclic amines, such as piperazine and its derivatives, have also attracted significant interest amongst crystal engineers, because they are able to form hydrogen bonds in multiple directions and are fairly rigid cations [14]. Furthermore, piperazine and its derivatives exhibit a wide range of biological activities including antimicrobial, anticancer, antituberculosis, antiviral and antimalarial activity [15]. In this context, we report herein the preparation of a new halogenocuprate complex $(C_6H_{16}N_2O)[CuCl_4]$, along with its X-ray crystal structure, Hirshfeld surface analysis, vibrational studies, density functional theory (DFT) calculations and antibacterial activity.

2. Experimental and calculations

2.1. Materials and physical measurements

The infrared spectrum of the title compound prepared as a KBR disk was recorded using a Nicolet IR 200 FT-IR spectrometer in the range 4000 - 400 cm^{-1}. Powder X-ray diffraction patterns were collected at room temperature in the 2θ range of 10-40° over 2 hours using a

BRUKER D8 ADVANCE X-ray diffractometer and graphite monochromated CuKα radiation.

2.2. Synthesis

The title compound, $(C_6H_{16}N_2O)[CuCl_4]$, was obtained as follows: a solution of N-(2-hydroxyethyl)piperazine (0.13 g, 1 mmol) in ethanol (10 mL) was added to a solution $CuCl_2.2H_2O$ (0.170 g, 1 mmol) in a minimum volume of ethanol. Concentrated hydrochloric acid (1 M, 20 mL) was also added dropwise to pH 1–1.5. The reaction mixture was stored in a water bath at 50°C for 1 hour. The resulting solution was kept at room temperature. After two weeks of evaporation, orange prismatic monocrystals appeared in the solution.

2.3. X-ray data collection

Single crystal X-ray diffraction data were collected on a Rigaku Oxford Diffraction SuperNova area-detector diffractometer using Mo Kα radiation (λ = 0.71073 Å) from a micro-focus X-ray source and an Oxford Instruments Cryojet XL cooler. Intensities were collected at 160 K by means of the CrysAlisPro software [16] and were corrected for Lorentz, and polarization effects. An empirical absorption correction using spherical harmonics was applied [17]. The structure was solved by direct methods with SHELXS-97 [18]. The molecular model was refined by full-matrix least-squares procedure on F^2 with SHELXL-2018 [19]. All methylene hydrogen atoms were positioned geometrically and refined using a "riding model" [with $U_{iso}(H) = 1.2U_{eq}(C)$]. The hydroxy and ammonium hydrogen atoms were located from difference *Fourier* maps and refined isotropically. A summary of the crystallographic data and the structure refinement results is given in **Table 1**. Crystallographic data for the structure reported in this paper have been deposited in the Cambridge Crystallographic Data Centre as supplementary publication number CCDC-1478572.The data can be obtained free of charge from http://www.ccdc.ac.uk/structures.

2.4. Computational details

The starting molecular geometry of $(C_6H_{16}N_2O)[CuCl_4]$ was taken directly from the refined crystal structure model. All calculations were performed using the Gaussian 09 package [20]. The optimization and vibrational frequency calculations of the title compound were carried out by using the Becke's three-parameter exchange functional combined with the Lee Yang Parr correlation functional (B3LYP) [21-22]. LanL2DZ was used as the basis set [23-25] as it has been found to yield good results for similar compounds [26-28]. The calculated vibrational wavenumbers were compared to the experimental counterparts. Vibrational mode assignments were made by comparison with previous theoretical and experimental results from analogous compounds [29-30] and by visual inspection of the modes animated by using the Gauss-View molecular visualization program [31].

The natural bond orbital (NBO) analysis of the title compound was carried out at the B3LYP/LanL2DZ level. The stabilization energies E(2) were computed by using second-order perturbation theory for examining the intermolecular interactions among the bonds of the investigated compound. The stabilization energy E(2) connected with electron delocalization between donor NBO(i) and acceptor NBO(j) was estimated with the following equation [32]:

$$E(2) = q_i \frac{(F_{ij})^2}{\square_j - \square_i}$$

where q_i is the donor orbital occupancy, ε_i, ε_j are diagonal elements (orbital energies) and F_{ij} is the off-diagonal NBO Fock matrix element.

2.5. Antibacterial activity determination

The inhibition efficiencies of the $(C_6H_{16}N_2O)[CuCl_4]$ salt were screened against the bacterial species Escherichia coli ATCC 8739, Salmonella typhimurium ATCC 14028, Staphylococcus aureus ATCC 6538, Enterococcus faecium ATCC 19434, Streptocoque B

(Streptococcus agalactiae), and Candida albicans ATCC 10231 by the disc diffusion method [33-35]. The test microorganisms were spread on suitable solid media plates and they were incubated for the whole night at 37°C. After one day, 4-5 loops of pure colonies were turned to a physiological saline solution in a test tube for every bacterial strain and then regulated to the 0.5 McFarland turbidity standards (*10^8 cells mL^{-1}). Sterile cotton dipped in the bacterial suspension and the agar plates were streaked three times. Each time, the plate was turned at a 60° angle. Finally, the swab was rubbed over the edge of the plate. Sterile filter paper discs Whatman (6 mm in diameter) were placed onto inoculated plates. These discs had previously been impregnated with diluted solutions of the $(C_6H_{16}N_2O)[CuCl_4]$ complex in sterile water to give a disc loading in the range of 50-250 µg. In the assay, Ampicillin (10µg/disc) was used as positive control for all strains while Nystatin (100µg/disc) was used for Candida albicans. The plates were incubated for 24 h at 37 °C and the results were determined by measuring the diameter of the inhibition zone around each disc. Each of the above tests was performed in duplicate.

3. Results and discussion

3.1. Crystal structure description

The experimental powder X-ray diffraction pattern (PXRD) of $(C_6H_{16}N_2O)[CuCl_4]$ is in good agreement with the simulated pattern derived from the model coordinates, indicating the purity and homogeneity of the synthesized product **(Fig. 1a)**. Minor differences in the positions, widths, and intensities of some peaks may be due to the different temperatures used for the single crystal (160 K) and powder diffraction measurements (room temperature), and preferred orientation effects with the powder samples [36]. Single-crystal X-ray diffraction analysis of crystals of the title complex showed the asymmetric unit to contain one discrete N-(2-hydroxyethyl)piperazine-1,4-diium dication and one discrete tetrachlorocuprate dianion (**Fig. 1b)**. The 6-membered piperazine ring adopts a chair conformation, as is evident from the

puckering parameters: Q=0.562 (4) Å, θ=2.7 (4)° and φ= 193 (8)° [37]. The interatomic C−C and C−N distances **(Table 2)** are comparable with values generally observed in other N-(2-hydroxyethyl)piperazine salts [30,38]. The Cu atom is coordinated by four almost equidistant Cl atoms in a geometry which is distorted significantly from tetrahedral towards a seesaw arrangement with a seesaw-typical τ_4 value of 0.68; τ_4 values range from 1.00 for an ideal tetrahedron to 0.0 for a square planar geometry [39]. In the crystal structure, the organic cations are interlinked via N−H···O hydrogen bonds to form extended chains, which run parallel to the [101] direction (**Table 3, Fig. 2a)** and can be described by a graphset motif of C(8) [40]. The anionic species interconnect the organic chains into a 3D famework by means of N−H···Cl and O−H···Cl hydrogen bonds (**Fig. 2b)**. Each cation interacts with four different anions and vice-versa. Each chlorine atom of the $[CuCl_4]^{2-}$anion is involved in only one hydrogen-bonding interaction, while one N-atom of the anion is involved in a bifurcated interaction with two different anions, N2−H2A···(Cl2^{iii}, Cl4^{iv}), although the interaction involving Cl4 is very much weaker than the others and has a rather sharp N−H···Cl angle (**Table 3**). These associations generate additional hydrogen-bonded ring motifs such as $R_3^3(11)$ and $R_5^5(23)$ [40]. The geometry of the ions of the fully optimized theoretical structure of the studied complex (**Table 2**) is very close to that exhibited by the crystal structure. The slight difference between the calculated and experimental distances and angles can be explained by the fact that the experimental values occur in the solid state, while the theoretical values correspond to the isolated ions in a vacuum.

3.2. Hirshfeld surface analysis

The intermolecular interactions of the tetrachlorocuprate salt can be visualized using Hirshfeld surface analysis [41]. The 3D Hirshfeld surface mapped over a d_{norm} range of -0.650 to 1.247Å is illustrated in **Fig.3**. **Fig.4** presents the 2D fingerprint maps which are unique for each entity in the asymmetric unit of a given crystal. The H···Cl and H···H intermolecular

contacts are the most abundant in the crystal packing (65.5% and 23.3% respectively) [42]. They have the most significant contribution to the total Hirshfeld surfaces. The Cl···H/H···Cl contacts, which are attributed to N−H···Cl and O−H···Cl hydrogen-bonding interactions, appear as two sharp symmetric spikes in the 2D fingerprint maps with a prominent long spike at de+di= 2.2 Å. The O···H/H···O contacts, that are attributed to H···O (de>di) and O···H (di>de) from N−H···O intercationic contacts, appear as two sharp symmetric spikes in the 2D fingerprint maps and account for 5.5% of the area of the Hirshfeld surface.

3.3.Vibrational spectra study

The simulated IR spectra of $(C_6H_{16}N_2O)[CuCl_4]$ performed with the B3LYP/LanL2DZ basis set and the experimental IR spectra are presented in **Fig. 5**. The experimental vibrational wavenumbers were correlated with the calculated vibrational wavenumbers and the correlation graph is shown in **Fig. 6**. The calculated correlation coefficient ($\mathbf{R^2}$) is 0.9999 for the studied compound. The calculated and experimental vibrational frequencies as well as the proposed assignments are collected in **Table 4**.

$[CuCl_4]^{2-}$ anion vibrational modes

The bands in the 311-233 cm^{-1} range are attributed to Cu−Cl stretching modes. The vibrational modes observed between 211 and 166 cm^{-1} are assigned to the Cu−Cl bending modes. The $CuCl_4$ bending vibrations appear at 118 and 103 cm^{-1}.

N-(2-hydroxyethyl)piperazine-1,4-diium cation vibrational modes

The symmetric and asymmetric stretching modes of NH_2 are observed at 3022 and 2913 cm^{-1}. The corresponding calculated values are 3005 and 2913 cm^{-1}. The bands assigned to the O−H and N−H stretching modes are found experimentally at 3300 and 2838 cm^{-1} (calculated at 3305 and 2824 cm^{-1}). The band located at 1636 cm^{-1} in the IR spectrum is assigned to the O−H in-plane deformation. The vibrational modes located between 1587 and 1219 cm^{-1} are attributed to the NH_2 and CH_2 bending modes. The bands in the 1160-1006 cm^{-1} range are

associated with the C−H, C−N and C−O stretching modes. Theoretically, these modes are observed between 1125 and 1006 cm^{-1}. The bands observed at 877 and 514 cm^{-1} are assigned to CCN and CCO bending, which are theoretically predicted at 871 and 519 cm^{-1}.

3.4.NBO analysis

The NBO analysis of the studied structure presents an efficient method for calculating the stabilization energies E(2) due to electron delocalization processes. **Table 5** presents the stabilization energies E(2), which indicate the electron delocalization from the donor NBO to acceptor [43,44]. The results indicate that the total stabilization energies of n(Cl3i) →σ*(N1−H1), n(Cl2ii) →σ*(N2−H1A) and n(Cl1) →σ*(O1−H11) interactions are, respectively, 14.64, 12.55 and 10.69 kcal/mol. These important interactions prove the existence of intermolecular N−H···Cl and O−H···Cl hydrogen-bonding interactions in the compound. Consequently, it is apparent that the N−H···Cl and O−H···Cl intermolecular interactions significantly influence crystal packing in this system.

3.5. Thermodynamic properties

Based on the vibrational analysis and statistical thermodynamics, the standard thermodynamic functions: heat capacity ($C_{p,m}^0$), enthalpy (H_m^0) and entropy (S_m^0), listed in **Table 6**, were obtained at the B3LYP/LanL2DZ level. From the table, these thermodynamic functions increase with temperature from 50 to 600 K, because the intensities of the molecular vibrations increase with temperature.

The correlation equations between thermodynamic properties and temperature T are as follows:

H_m^0= -2,58341+ 0,07224T + 7,96114T^2 x 10^{-4} ; (R^2=0,99988)

$C_{p,m}^0$= 48,39318+ 0,31818T-2,2596T^2 x 10^{-4} ; (R^2= 0,98627)

S_m^0= 96,97318+ 0,78837 T- 5,35958 T^2 x 10^{-4} ; (R^2= 0,99637)

3.6. Antibacterial activity

The elaborated copper complex was screened for antibacterial and antifungal activity against three gram-positive bacteria (E. coli, S. typhimurium, S.aureus), two gram-positive bacteria (E. faecium and S. agalactiae) and against fungi (Candida albicans). The susceptibility of the bacteria and fungi strains toward the copper complex was screened by measuring the diameter of the growth inhibition zone. The results reported in **Table 7**, indicate that the synthesized compound exhibited varying degrees of inhibitory effect on the growth of different tested strains. Compared to reference drugs, the tested compound exhibited moderate activity against the gram-negative bacteria, while it showed modest activity against the fungal and the gram-positive strains, except for S. aureus.

4. Conclusion

The present work investigates the synthesis and subsequent characterization of a new compound $(C_6H_{16}N_2O)[CuCl_4]$. Single crystal X-ray diffraction showed the presence of one-dimensional N−H···O hydrogen-bonded chains linking the organic cations. This chain interconnects the anionic species into a three-dimensional framework by means of N−H···Cl and O−H···Cl hydrogen bonds. Reproduction of the molecular geometry and FT-IR vibrational spectra of the title compound, as well as an NBO analysis were carried out by using the density functional method (B3LYP) with the Lanl2DZ basis set. The calculated results show that the optimized geometry can well reproduce the crystal structure, and the theoretical vibrational wavenumbers values are in agreement with experimental values. The correlations between the thermodynamic properties H_m^0 , $C_{p,m}^0$, S_m^0 and temperature were obtained. The NBO analysis indicated that the N−H···Cl and N−H···Cl intermolecular interactions significantly influence crystal packing in this system.

Acknowledgments

This work has been supported by the Ministry of Scientific Research and Development of Tunisia.

References

[1]K. Sakai, M. Takemura, Y. Kawabe, Lead chloride-based layered perovskite incorporated with an excited state intramolecular proton transfer dye, J. Lumin.130 (2010) 2505-2507.

[2]K. Pradeesh, G. S. Yadav, M. Singh, G. V. Prakash, Synthesis, structure and optical studies of inorganic–organic hybrid semiconductor, $NH_3(CH_2)_{12}NH_3PbI_4$, Mater. Chem. Phys. 124 (2010) 44-47.

[3]M. Zdanowska-Fraczek, K. Holderna-Natkaniec, Z.J. Fraczek, R. Jakubas, Molecular dynamics and electrical conductivity of $(C_3N_2H_5)_5Bi_2Cl_{11}$, Solid State Ion. 180 (2009) 9-12.

[4]I.Chaabane, F. Hlel, K. Guidara, Dielectric spectroscopy study of the new compound $[C_{12}H_{17}N_2]_2CdCl_4$, J. Alloys Compd. 461 (2008) 495-500.

[5]K. Karoui, A.B. Rhaiem, K. Guidara, Dielectric properties and relaxation behavior of $[TMA]_2Zn_{0.5}Cu_{0.5}Cl_4$ compound, Phys. B. 407 (2012) 489-493.

[6]M. Bujak, J. Zaleski, High temperature ferro-paraelectric phase transition in tris(trimethylammonium) nonachlorodiantimonate(III) (TMACA) studied by X-ray diffraction method, Cryst. Eng. 4 (2001) 241-252.

[7]Vishwakarma, P. Ghalsasi, A. Navamoney, Y. Lan, A. Powell, Structural phase transition and magnetic properties of layered organic‑inorganic hybrid compounds: *p*-Haloanilinium tetrachlorocuparate(II), Polyhedron 30 (2011) 1565-1570.

[8]F. Issaoui, I. baccar, O. El Sadek, F. Zouari, E. Dhahri, E. K. Hlil, Physical Properties and Electronic Structure Study of the 1-(2-aminoethyl)

Piperaziniumtrichlorocuprate (II) Monohydrate, J. Supercond. Nov. Magn. **25**(2012)1563–1570.

[9]P. S. Subramanian, D. Srinivas, Synthesis, spectral characterization and magnetic properties of dicarboxylato-bridged dinuclear copper(II) complexes with n-pyridylsalicylidenaminato ligand, Polyhedron 15 (1996) 985-989.

[10]S. V. Voitekhovich, A. S. Lyakhov, L. S. Ivashkevich, F. Schleife, R. Schnorr, B. Kersting, P. N. Gaponik, Synthesis and characterization of 5-amino-1,3-di-tert-butyl-2H-tetrazol-1-iumbis[di-μ-chlorido-bis[dichloridocuprate(II)]], Inorg. Chim. Acta 419 (2014) 124-129.

[11]R. D. Willett, C. J. Gomez-Garcia, B. Twamley, Structure and magnetic properties of $[(REDA)Cl]_2CuCl_4$ salts: A new series of ferromagnetic layer perovskites, Polyhedron 24 (2005) 2293-2298.

[12]I. Baccar, F. Issaoui, F. Zouari, M. Hussein, E. Dhahri, M. A. Valente, Magneto-structural studies of the bis (1,4-bis (3-aminopropylamine) piperazinium) chloride pentachlorocuprate (II) trihydrate, Solid State Commun. 150 (2010) 2005-2010.

[13]S. Bouacida,R.Bouchene, A. Khadri, R. Belhouasa, H.Meraziga, Bis[4-(dimethylamino)pyridinium] tetrachloridocuprate(II), Acta Crystallogr,. Sect. E, 69 (2013) m610–m611.

[14] C. S. Hawes, C. Chen, A. Tran, D. R. Turner, Hydrogen-Bonding Motifs in Piperazindiium Salts, Crystals 4 (2014) 53-63.

[15]N. Prabavathi, A. Nilufer, V. Krishnakumar, FT-IR, FT-Raman and DFT quantum chemical study on the molecular conformation, vibrational and electronic transitions of 1-(m-(trifluoromethyl)phenyl)piperazine, Spectrochim. Acta A 121 (2014) 483–493.

[16]CrysAlisPro, Version 1.171.38.41r, Rigaku Oxford Diffraction, Abingdon, Oxfordshire, England, 2015.

[17]R. H. Blessing, An empirical correction for absorption anisotropy, Acta Crystallogr., Sect. A: Found. Crystallogr., 51 (1995)33-38.

[18]G. Sheldrick, A short history of SHELX, Acta Crystallogr., Sect. A: Found.Crystallogr., 64 (2008) 112-122.

[19]Crystal structure refinement with SHELXL, Acta Crystallogr., Sect. C: Struct. Chem. 71 (2015) 3-8.

[20]M. J.Frisch, G. W. Trucks, H. B. Schlegel, G. E. Scuseria, M. A. Robb, J. R. Cheeseman, G. Scalmani, V. Barone, B. Mennucci, G. A. Petersson, Gaussian, Inc.,Wallingford CT, 2009.

[21]A. D. Becke, Density-functional thermochemistry. III. The role of exact exchange, J. Chem. Phys. 98 (1994) 5648-5652.

[22]P. J. Stephens, F. J. Devlin, C. F. Chabalowski, M. J. Frisch, Ab Initio Calculation of Vibrational Absorption and Circular Dichroism Spectra Using Density Functional Force Fields J. Phys. Chem. 98, (1994) 11623-11627.

[23]P. J. Hay, W. R. Wadt, Ab initio effective core potentials for molecular calculations. Potentials for the transition metal atoms Sc to Hg, J. Chem. Phys. 82 (1985)270-283.

[24] N. Zhanpelsov, M. Matsuoka, H. Yamashite, M. Anpo, Cluster quantum chemical ab initio study on the interaction of NO molecules with highly dispersed titanium oxides incorporated into silicalite and zeolites, J. Phys. Chem. B.102 (1998) 6915-6920.

[25]N. Niclasc, M. Dolg, H. Stoll, H. Preuss, Ab initio energy-adjusted pseudopotentials for the noble gases Ne through Xe: Calculation of atomic dipole and quadrupole polarizabilities, J. Chem. Phys. 102 (1995) 8942-8953.

[26]S. Chaouachi, S. Elleuch, B. Hamdi, R. Zouari, Experimental (FTIR, Raman, UV–visible and PL) and theoretical (DFT and TDDFT) studies on bis(8–hydroxyquinolinium) tetrachlorocobaltate(II) compound, J. Mol. Struct. 1125 (2016) 149-161.

[27] R. Mesbeh, B. Hamdi, R. Zouari, Crystal structure, thermal studies, Hirshfeld surface analysis, vibrational and DFT investigation of organic-inorganic hybrid compound $[C_9H_6NOBr_2]_2CuBr_4.2H_2O$, J. Mol. Struct. 1125 (2016) 217-226.

[28] A. Tounsi, S. Elleuch, B. Hamdi, R. Zouari, A. Ben Salah , Structural study, Hirshfeld surface analysis, spectroscopic properties and DFT investigation of a new hybrid compound: $(C_6H_{10}(NH_3)_2)_3[CoCl_4](Cl)_4.3H_2O$, J. Mol. Struct.1141 (2017) 512-523.

[29] Z. Aloui, V. Ferretti, S. Abid, M. Rzaigui, F. Lefebvre, M. Ben Nasr, Synthesis, crystal structure and characterization of a new organic-inorganic hybrid material: $[C_6H_{16}N_2O]SbCl_5$, J. Mol. Struct.1087 (2015) 26-32.

[30]S. Soudani, E. Jeanneau, C. Jelsch, F. Lefebvre, C. Ben Nasr, A Hirshfeld surface analysis, crystal structure and physicochemical studies of zwitterionic complex: 1-(2-hydroxyethyl)piperaziniumtrichlorozincate (II), Inorg. Chem. Comm. 70 (2016) 65-70.

[31] R. Dennington II, T. Keith, J. Millam, Gauss View, Version 4.1.2, Semichem. Inc. Shawnee Mission, KS, (2007).

[32]E. Scrocco, J. Tomasi, Electronic Molecular Structure, Reactivity and Intermolecular Forces: An Euristic Interpretation by Means of Electrostatic Molecular Potentials, Adv. Quantum Chem**.** 11(1978) 115-193.

[33]G. Tadesse, E. Ephraim, M. Ashenafi, Assessment of the antimicrobial activity of lactic acid bacteria isolated from Borde and Shamita, traditional Ethiopian fermented beverages, on some food borne pathogens and effect of growth medium on the inhibitory activity, Int. J. Food Saf. 5 (2005)13-20.

[34]O. Y. Celikatas, E. Bendir, and F. V. Sukan, In vitro antioxidant activities of Rosmarinus officinalis extracts treated with supercritical carbon dioxide, Food Chem. 101 (2007) 1457-1464.

[35]G. Sacchetti, S. Maietti, M. Muzzoli, M. Scaglianti, S. Manfredini, M. Radice, R. Bruni, Comparative evaluation of 11 essential oils of different origin as functional antioxidants, antiradicals and antimicrobials in foods, Food Chem. 91 (2005) 621-632.

[36]Z. B. Han, Y. K. He, C. H. Ge, J. Ribas, L. Xu, Hydrothermal syntheses, crystal structures and magnetic properties of two copper(II) complexes involved in situ ligand synthesis, Dalton Trans, 28 (2007) 3020-3024.

[37]D. Cremer, J. A. Pople, General definition of ring puckering coordinates, J. Am. Chem. Soc. 97 (1975)1354–1358.

[38]Z. Aloui, V. Ferretti, S. Abid, M. Rzaigui, F. Lefebvre, M. Ben Nasr, Synthesis, crystal structure and characterization of a new organic-inorganic hybrid material: $[C_6H_{16}N_2O]SbCl_5$, J. Mol. Struct.1087 (2015) 26-32.

[39]L. Yang, R. D. Powell, P. R. Houser, Structural variation in copper(I) complexes with pyridylmethylamide ligands: structural analysis with a new four-coordinate geometry index, τ4, Dalton Trans. 9 (2007) 955–964.

[40]J. Benstein, RE. Davis, L. Shimoni, N-L Chang, Patterns in Hydrogen Bonding: Functionality and Graph Set Analysis in Crystals, Angew. Chem. Int. Ed. Engl. 34 (1995)1555-73.

[41]S. K. Wolff, D. J. Grimwood, J. J. McKinnon, D. Jayatilaka, M. A. Spackamn, Crystal Explorer, University of Western Australia (2012).

[42]C. F. Matta, J. Hernandez-Trujillo, T. H. Tang, R. F. W. Bader, Hydrogen-Hydrogen Bonding: A Stabilizing Interaction in Molecules and Crystals, Chem. Eur. J. 9 (2003) 1940-1951.

[43]Sebastian, N. Sundaraganesan, The spectroscopic (FT-IR, FT-IR gas phase, FT-Raman and UV) and NBO analysis of 4-Hydroxypiperidine by density functional method, Spectrochim. Acta A, 75 (2010) 941-952.

[44]J. Hubert, I. Kostova, C. Ravikumar, M. Amalanathan, S. C. Pinzaru, Theoretical and vibrational spectral investigation of sodium salt of acenocoumarol, J. Raman Spectrosc.40 (2009) 1033-1038.

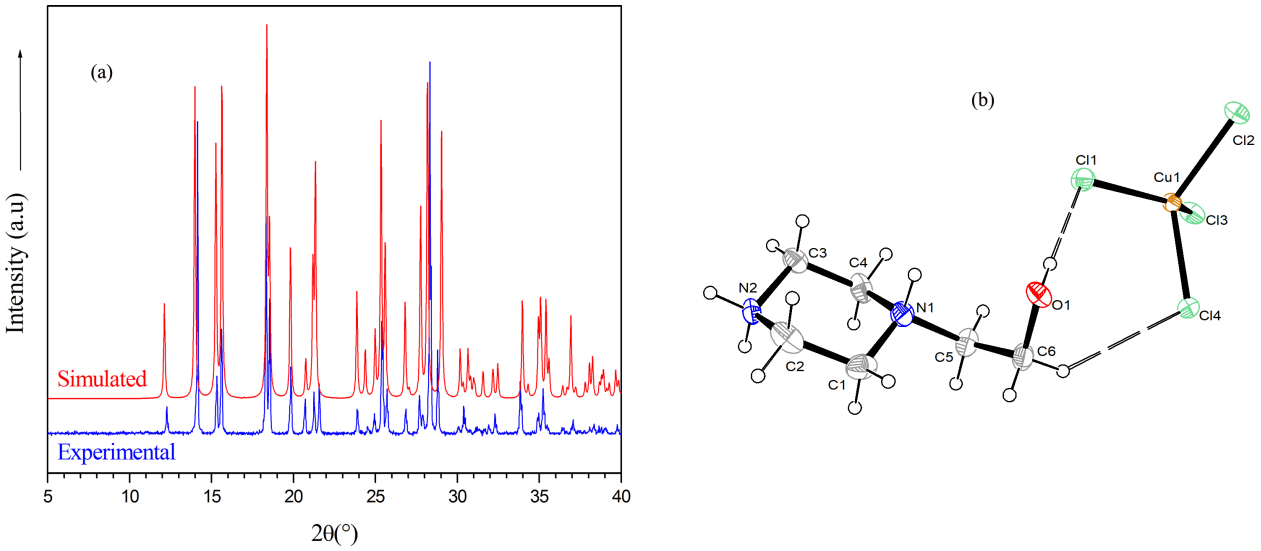

Fig.1. (a) Simulated and experimental powder X-ray diffraction patterns of $(C_6H_{16}N_2O)[CuCl_4]$. **(b)**Asymmetric unit of $(C_6H_{16}N_2O)[CuCl_4]$with the atom numbering scheme and displacement ellipsoids at 50 % probability.

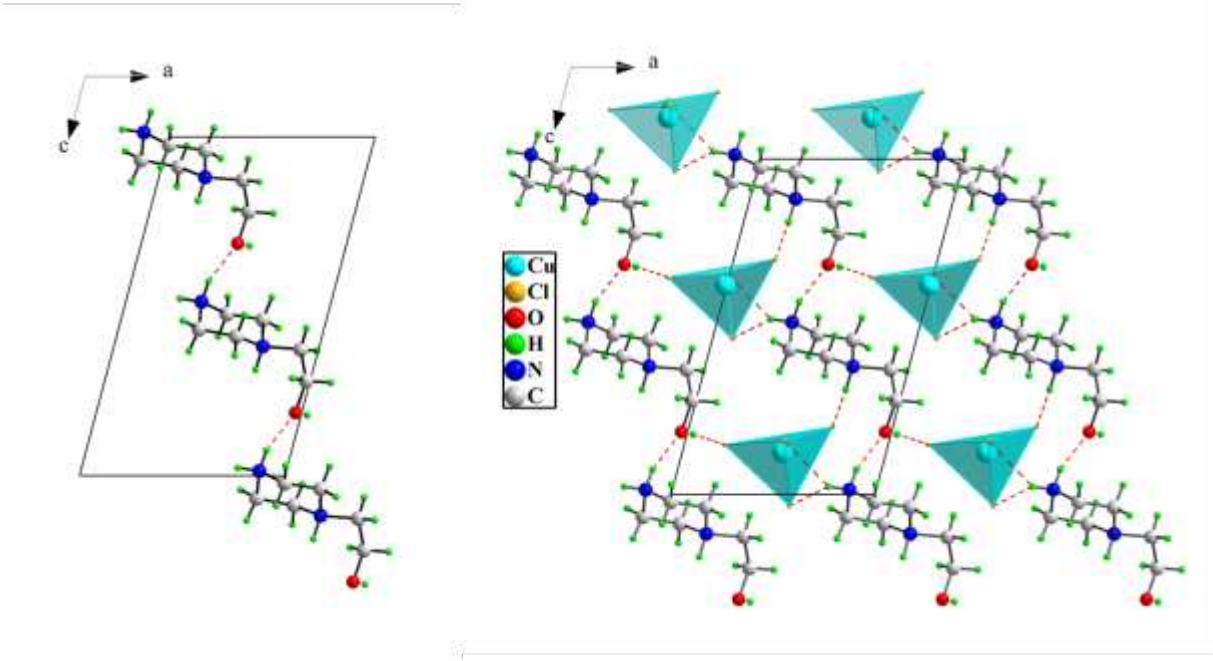

Fig.2. (a) View of the 1D cationic chain running along the [101] direction formed by the N–H···O interactions. **(b)** Projection of the crystal structure of $(C_6H_{16}N_2O)[CuCl_4]$ in the (ac) plane showing the N–H···O, N–H···Cl and O–H···Cl hydrogen bonds.

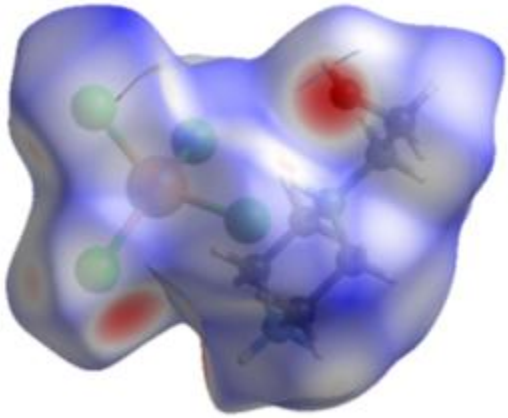

Fig.3. Hirshfeld surface mapped over d_{norm} of $(C_6H_{16}N_2O)[CuCl_4]$.

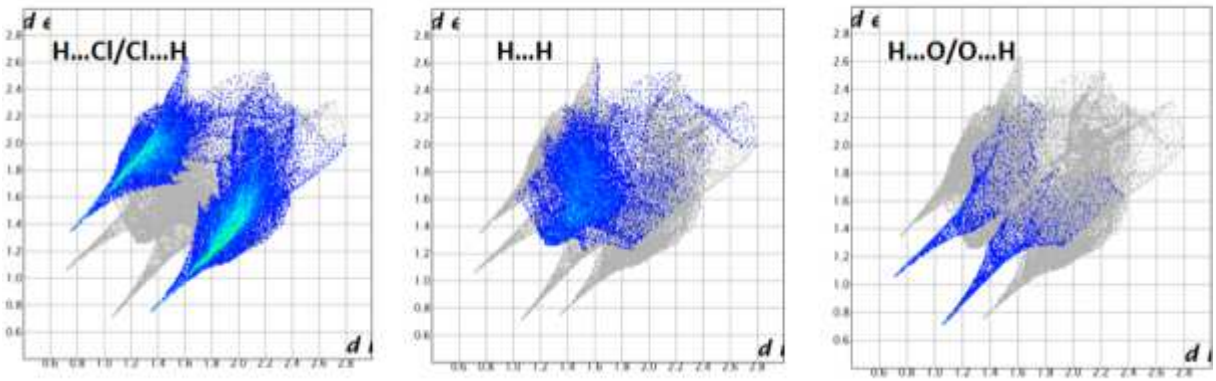

Fig.4. Two-dimensional fingerprint plots for $(C_6H_{16}N_2O)[CuCl_4]$ showing contributions from different contacts.

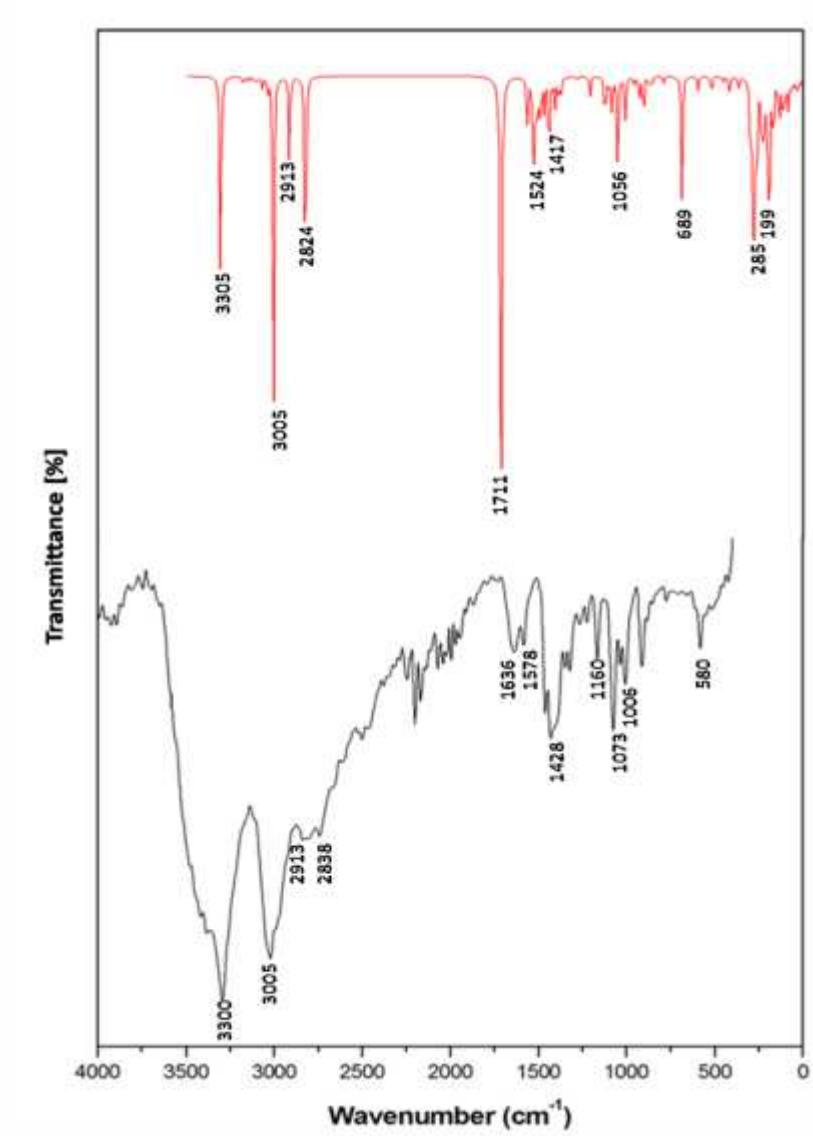

Fig.5. (a) Simulated and **(b)** experimental IR spectrum of $(C_6H_{16}N_2O)[CuCl_4]$.

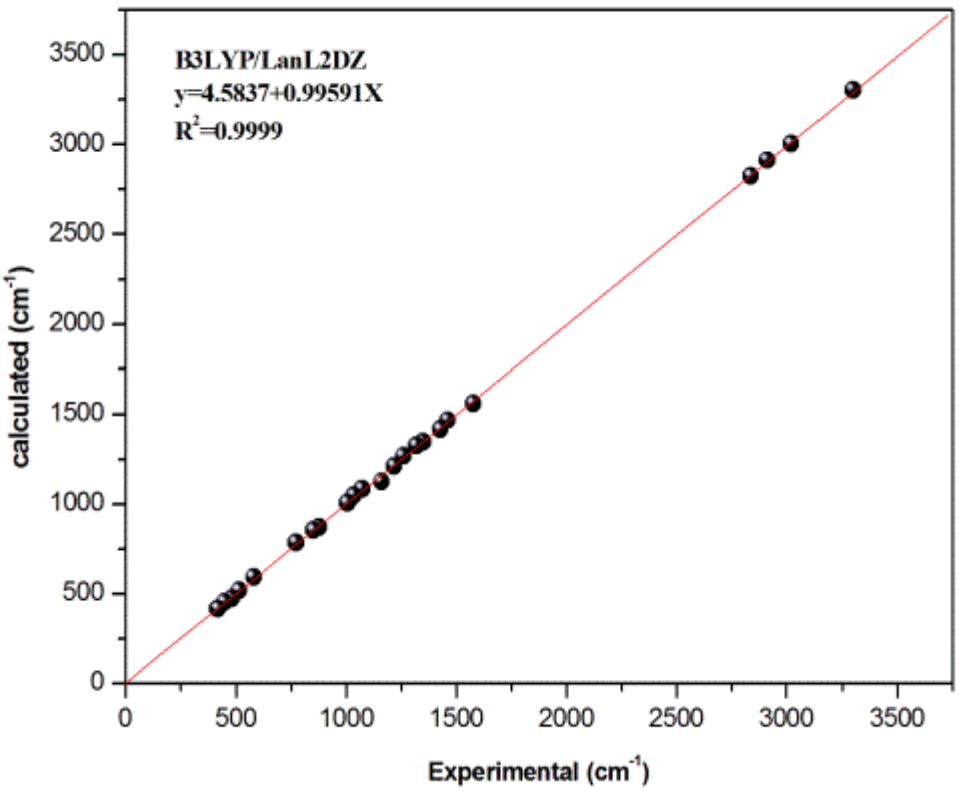

Fig.6. Correlation graph between the experimental and calculated wavenumbers (cm^{-1})